Available online at www.sciencedirect.com

SciVerse ScienceDirect

Geochimica et Cosmochimica Acta 105 (2013) 1–13

Geochimica et Cosmochimica Acta

www.elsevier.com/locate/gca

Na-bearing majoritic garnet in the $Na_2MgSi_5O_{12}$–$Mg_3Al_2Si_3O_{12}$ join at 11–20 GPa: Phase relations, structural peculiarities and solid solutions

Anna M. Dymshits [a,b], Andrey V. Bobrov [c,*], Luca Bindi [d,e], Yuriy A. Litvin [f], Konstantin D. Litasov [b,g], Anton F. Shatskiy [b,g], Eiji Ohtani [g]

[a] *Vernadsky Institute of Geochemistry and Analytical Chemistry, Ul. Kosygina 19, 119991 Moscow, Russia*
[b] *Sobolev Institute of Geology and Mineralogy, Siberian Branch, Russian Academy of Sciences, Prosp. Ak. Koptyuga 3, 630090 Novosibirsk, Russia*
[c] *Geological Faculty, Moscow State University, Leninskie Gory, 119991 Moscow, Russia*
[d] *Dipartimento di Scienze della Terra, Università di Firenze, Via La Pira 4, I-50121 Firenze, Italy*
[e] *C.N.R., Istituto di Geoscienze e Georisorse, Sezione di Firenze, Via La Pira 4, I-50121 Firenze, Italy*
[f] *Institute of Experimental Mineralogy, Russian Academy of Sciences, Chernogolovka, 142432 Moscow, Russia*
[g] *Department of Earth and Planetary Materials Science, Graduate School of Science, Tohoku University, Sendai 980-8578, Japan*

Received 24 May 2012; accepted in revised form 20 November 2012; available online 3 December 2012

Abstract

Na-majorite $Na_2MgSi_5O_{12}$ (NaMaj), an end-member of sodium-rich majoritic garnet, was synthesized and garnet/pyroxene transition was studied in Kawai-type multi-anvil experiments at 11–20 GPa and 1500–2300 °C. Na-majorite was obtained at 16 GPa and 1500 °C; its stability spreads to the high-temperature region with pressure (1900 °C at 17 GPa and 2100 °C at 19.5 GPa). Experimental study of the $Mg_3Al_2Si_3O_{12}$ (Prp)–$Na_2MgSi_5O_{12}$ join at 11–20 GPa demonstrated the following phase assemblages changing with pressure: garnet + two pyroxenes (enstatite-rich and Na-pyroxene); garnet + pyroxene (enstatite–jadeite–Na-pyroxene) + stishovite; garnet + stishovite; garnet + $NaAlSiO_4$ with calcium ferrite-type structure + stishovite. For a given bulk composition ($Prp_{50}NaMaj_{50}$), a regular increase of both Na and Si concentrations and consequently, NaMaj mole portion in garnets was observed. From 8.5 to 20 GPa, the concentration of Na_2O increased from 1.52 to 5.71 wt.%, which correspond to a NaMaj content of ~40 mol.%. The highest Na_2O content (12.24 wt.%) was registered at 18.5 GPa and 1600 °C for the $Prp_{20}NaMaj_{80}$ starting composition. Experiments at 18.5 GPa and 1600 °C on the pyrope–Na-majorite join allowed us to study mixing peculiarities for sodium-rich majoritic garnet. The transition from cubic (*Ia3d*) to tetragonal ($I4_1/acd$) symmetry was observed for the composition with ~80 mol.% $Na_2MgSi_5O_{12}$, which is consistent with the similar change of the structure in the pyrope–majorite ($Mg_4Si_4O_{12}$) system. Significant Na-majorite solubility in pyrope, as well as findings of natural garnets with high Na concentrations (>1 wt.% Na_2O) allow us to consider Na-bearing majoritic garnet as an important concentrator of sodium in the deep upper mantle and transition zone.

1. INTRODUCTION

Data on the composition of deep-seated rocks and minerals are widely applied for substantiation of concepts on the phase composition and structure of the Earth's interior. Over the last decades, ultrahigh-pressure minerals, such as $MgSiO_3$ with presumable ilmenite and perovskite

* Corresponding author. Present address: Department of Petrology, Geological Faculty, Moscow State University, Leninskie Gory, 119991 Moscow, Russia. Tel.: +7 495 939 4929; fax: +7 495 932 8889.
E-mail address: archi@geol.msu.ru (A.V. Bobrov).

0016-7037/$ - see front matter © 2012 Elsevier Ltd. All rights reserved.
http://dx.doi.org/10.1016/j.gca.2012.11.032

structures, $CaSiO_3$ with perovskite structure, magnesiowustite (ferropericlase), and majoritic garnet were discovered as inclusions in diamonds (Moore and Gurney, 1985; Harte et al., 1999; Stachel et al., 2000; Stachel, 2001; Kaminsky, 2012).

Among the mentioned phases majoritic garnet is the only one, which retains its structural features at decreasing pressure. The composition of this mineral indicates thermodynamic parameters of its formation (Akaogi and Akimoto, 1977; Irifune, 1987) attracting interest of petrologists and experimentalists. Majoritic garnet is an important mineral phase in the lowermost upper mantle and the transition zone of the Earth at depths of 300–660 km. Under these conditions, the garnet phase makes up ~40 vol.% for peridotitic compositions and as much as 60 vol.% for basaltic or eclogitic compositions (e.g., Ringwood, 1991). Some experiments demonstrated that majorite is stable under pressures of up to 28 GPa (Irifune and Ringwood, 1993; Litasov et al., 2004); and the association of majorite, in diamond from the Juina placers in Brazil, with perovskite and ilmenite (Wilding et al., 1991; Kaminsky et al., 2001) allows also to assume its presence in the uppermost horizons of the lower mantle.

The composition of eclogitic and peridotitic garnets in mantle rocks including diamondiferous xenoliths and inclusions in diamonds may be expressed by a general formula $\{X^{2+}\}_3[Y^{3+}]_2(Si)_3O_{12}$, where {X} dodecahedral site is occupied by divalent cations (mainly Mg, Ca, Fe^{2+}, Mn); octahedral [Y] site is filled with trivalent cations (Al, Cr, Fe^{3+}); (Si) is present in tetrahedra reaching three cations for twelve oxygen atoms (or for eight total cations). With increasing depth up to 300 km and more (Ringwood and Major, 1971; Akaogi and Akimoto, 1979; Irifune et al., 1986; Irifune, 1987), garnet becomes progressively depleted in Al and Cr; Si content in octahedral [Y] site, as well as concentrations of divalent cations X^{2+} (Ca, Mg, Fe) and Na, regularly increase (Ono and Yasuda, 1996). Such garnets are traditionally denoted as *majoritic*, which form complex solid solutions between cubic garnet and the components $\{Mg\}_3[Mg, Si]_2(Si)_3O_{12}$ and $\{Ca, Mg\}_3[Mg, Si]_2(Si)_3O_{12}$ (at low pressures they are represented by enstatite $MgSiO_3$ and diopside $CaMgSi_2O_6$, respectively). With regard to microprobe analysis error, Gasparik (2002) suggested to attribute garnets to majoritic type, if Si concentration in them exceeds 3.03 formula units. Methods of depth estimation based on the composition of majoritic garnet were developed (e.g., Collerson et al., 2010) including semi-quantitative Na-in-garnet barometer (Simakov and Bobrov, 2008).

One particular feature of majorite is an isomorphic sodium admixture being registered both in natural and experimentally synthesized garnets. Sodium admixture in natural majoritic garnets was originally discovered by Sobolev and Lavrent'ev (1971). They studied garnets from diamonds, diamond-bearing eclogites and metamorphic rocks of high-pressure complexes and measured 0.09–0.22 wt.% Na_2O in garnets from diamond-bearing eclogites suggesting a link with pressure. This is due to the fact that Na incorporation in garnet requires the transition of some silicon to the octahedral site according to the heterovalent substitution $^{VIII}(Mg^{2+},Ca^{2+},Fe^{2+}) + {}^{VI}Al^{3+} \rightarrow {}^{VIII}Na^{+} + {}^{VI}Si^{4+}$. Later majoritic garnets with higher sodium concentrations were discovered in many regions worldwide (Stachel, 2001) including Kankan area in Guinea, West Africa (Stachel et al., 2000), where majorite with the highest sodium content (1.37 wt.% Na_2O) is associated with potassium-rich clinopyroxene (1.44 wt.% K_2O). Recently Harte and Cayzer (2007) described exsolution textures of clinopyroxene in majoritic garnet indicating the initial sodium concentration of 2.16 wt.% Na_2O.

Conditions of formation, structural features, and composition of majoritic garnets were studied in numerous experiments for simple model systems (Akaogi and Akimoto, 1977; Gasparik, 1989, 1992, 1996, 2002), as well as multicomponent systems with natural chemistry (Irifune et al., 1986; Irifune, 1987; Ono and Yasuda, 1996; Litasov and Ohtani, 2005). However, the physicochemical behavior of sodium components of minerals in magmatic processes under mantle pressures and temperatures is not well studied. Experiments in the systems with Na_2O content exceeding 3.5 wt.% (the upper boundary of alkalinity for MORB) at 4–22 GPa (e.g., Gasparik, 1996; Bobrov et al., 2008a) demonstrate that irrespective of initial parities of the components in starting materials, Al content decreases whereas Si and Na concentrations increase with pressure (Fig. 1).

Our recent experiments in the model system pyrope $Mg_3Al_2Si_3O_{12}$–sodium majorite $Na_2MgSi_5O_{12}$ (NaMaj) under *P*–*T*-conditions of the diamond formation (7.0 and 8.5 GPa) (Bobrov et al., 2008b) show that garnet (Grt) occurs on liquidus of the system (40–60 mol.% Prp in starting materials) at $T < 1900$ °C. When the temperature decreases to 1750 °C, garnet is accompanied by enstatite (En) phenocrysts, and sodium-rich starting compositions produce coesite and sodium pyroxene ($NaMg_{0.5}Si_{2.5}O_6$) (NaPx) at $T = 1700$°C. Four-phase assemblage (Grt + NaPx + En + Melt) was observed at $T \approx 1600$ °C. The experiments allowed identification of stable sodium admixture in garnet (0.3–0.6 wt.% Na_2O) being controlled by temperature and pressure. The highest sodium concentrations of >1.5 wt.% Na_2O (~12 mol.% of $Na_2MgSi_5O_{12}$) were obtained at $P = 8.5$ GPa near the solidus of the system.

X-ray diffraction studies of solid solutions along the majorite (Maj)–pyrope (Prp), $Mg_4Si_4O_{12}$–$Mg_3Al_2Si_3O_{12}$, join have shown that majorite garnet undergoes a phase transformation from cubic to tetragonal symmetry at Prp_{25}-Maj_{75} (Table 1). The observed changes of unit-cell parameters, although slightly different in various studies (Akaogi and Akimoto, 1977; Parise et al., 1996; Heinemann et al., 1997), are monotonous increasing linearly with increasing amount of $Mg_4Si_4O_{12}$ and show no obvious discontinuities close to the change over from cubic to tetragonal. There were no data on the study of solid solutions along the pyrope–sodium majorite join.

Our experiments were aimed on the study of phase relations and synthesis of solid solutions of Na-bearing majoritic garnet in the system $Na_2MgSi_5O_{12}$–$Mg_3Al_2Si_3O_{12}$ at 11–20 GPa and 1500–2300 °C modeling the conditions of the lowermost upper mantle and transition zone. The garnet/pyroxene transition for sodium-rich compositions is discussed as well.

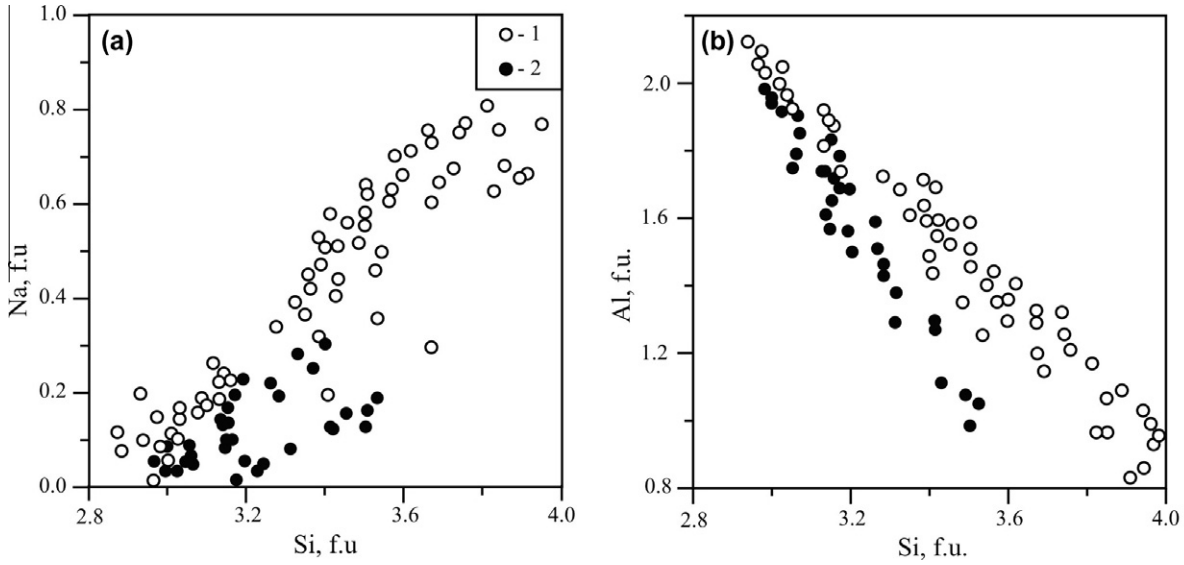

Fig. 1. Compositional variations in majoritic garnets synthesized in experiments at 10–22 GPa (1), after (Irifune et al., 1986; Gasparik, 1996; Ono and Yasuda, 1996; Bobrov et al., 2008a), in comparison with the data on inclusions in natural diamonds (2), after (Moore and Gurney, 1985; Davies et al., 1999, 2004; Stachel, 2001; Pokhilenko et al., 2004; Harte and Cayzer, 2007; Shatskii et al., 2010). The difference between the experimental and natural data at high Si contents is explained by relative enrichment in Si ($Mg_4Si_4O_{12}$) and depletion in Na ($Na_2MgSi_5O_{12}$) for natural majoritic garnets, which is consistent to the low-Na bulk compositions.

Table 1
Lattice parameters of garnets on the join majorite–pyrope.

Majorite (mol.%)	Parise et al. (1996)		Heinemann et al. (1997)		Akaogi and Akimoto (1977)
	a (Å)	*c* (Å)	*a* (Å)	*c* (Å)	*a* (Å)
0	11.452		11.456		
5					11.459
18					11.463
25			11.464		
40	11.468				11.465
48	11.473		11.471		11.469
59					11.472
74	11.478		11.476		11.473
80	11.494	11.457	11.480	11.475	
87			11.496	11.458	
93			11.509	11.442	
100	11.515	11.429	11.519	11.420	

2. EXPERIMENTAL AND ANALYTICAL TECHNIQUES

Mixtures of stoichiometric gels of pyrope, $Mg_3Al_2Si_3O_{12}$, and $Na_2MgSi_5O_{12}$ compositions were used as starting materials. The gels were prepared using the nitrate gelling method (Hamilton and Henderson, 1968). Starting mixtures of desired bulk compositions were homogenized at a room temperature using ethanol and then dried in the stove at 400 °C. All cell assembly details and gaskets were also dried in the oven to prevent possible hydrogen penetration.

Experiments were performed at $P = 11$–20 GPa and $T = 1500$–2300 °C using 1500 and 3000 ton Kawai-type multianvil apparatus at Tohoku University, Sendai, Japan. The truncated edge lengths of the WC anvils were 5.0 and 3.5 mm depending on pressure. Octahedral cell assemblage with edge lengths of 9.9 and 11.4 mm was manufactured from semi-sintered zirconia. The dimension of the pyrophyllite gaskets surrounding the cell assembly was 3.0–4.0 mm. The sample was loaded into platinum or rhenium capsules isolated from cylindrical $LaCrO_3$ heater by BN spacer. Every sample contained two charges: one of them with pure Na-majorite gel and another with Na-majorite–pyrope mixture (Fig. 2a). Special experimental series was performed using a large volume cell, which allowed us to study eight starting compositions in one run (Frost et al., 2004; Shatskiy et al., 2011). The pressure media made of Cr-doped MgO were shaped as octahedra with an edge length of 14 mm. Two molybdenum capsules with samples were separated by thermocouple and isolated from the central part of the $LaCrO_3$ heater by zirconia spacers (Fig. 2b).

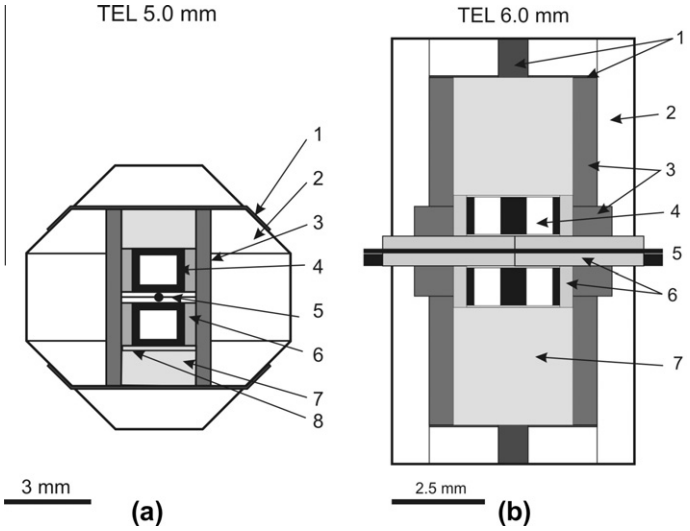

Fig. 2. The furnace assemblies used for experiments in this study. (1) Mo electrodes; (2) pressure medium (ZrO_2); (3) $LaCrO_3$ heater; (4) Mo sample capsule; (5) W–Re thermocouple; (6) BN (a) and ZrO_2 (b) spacers; (7) MgO insulators; (8) pressure marker.

Temperature was measured using a $W_{97}Re_3$–$W_{75}Re_{25}$ thermocouple located at the center of the cell assembly. As was demonstrated by Litasov and Ohtani (2009), the lateral temperature variations across charge did not exceed 50 °C. Press loading was calibrated based on *in situ* synchrotron X-ray diffraction experiments at "Spring-8" facility by the Au pressure scale (Fei et al., 2007), similarly to Litasov and Ohtani (2009). The relative uncertainty in pressure was estimated to be smaller than ±1 GPa. In addition, pressure calibration was confirmed by phase transitions in $MgSiO_3$ and Mg_2SiO_4 placed inside the heater under the sample capsule. The stable phases were identified by Raman spectroscopy and showed good agreement with pressure calibration obtained by *in situ* methods. Durations of individual runs varied from 30 to 1440 min (24 h).

Each run sample was divided into several pieces for microprobe analysis and XRD measurements. To analyze phase compositions on an energy-dispersive electron microprobe, the samples were embedded into epoxy and polished. Compositions of synthesized phases were studied in the Laboratory of Local Methods of Matter Study, Geological Faculty, Moscow State University, by using a Jeol JSM-6480LV electron microscope equipped with an energy-dispersive electron microprobe INCA Energy. Na-majorite–pyrope solid solutions were studied on a scanning electron microscope CamScan MV2300 (VEGA TS 5130MM) equipped with the EDS electron microprobe Link INCA Energy at the RSMA laboratory of the Institute of Experimental Mineralogy. The following standards were used: synthetic SiO_2, MgO, and Al_2O_3 for Si, Mg, and Al, respectively, and natural albite for Na. The ZAF matrix correction was used. Phase compositions in each run were determined from the average of 2–6 analyses performed at 15 and 20 kV accelerating voltage, 15 and 10 nA beam current. The main criterion for considering the pyroxene or garnet analyses acceptable was the sum of cations for 6 oxygens being between 3.98 and 4.02. Microprobe analyses of the quenched melt were made using a defocused beam scanning an area of 10 × 10 μm. No significant differences in sample textures and mineral composition were observed for the runs with different durations thus confirming that the chemical equilibrium was achieved in the runs, even for subsolidus conditions.

Identification of phases in experimental samples was performed on a microfocus diffractometer M18XCE (MacScience Co. Ltd.) at Tohoku University by X-ray patterns obtained in CrKα monochromatic radiation (37 kV, 70 mA). Several crystals of Na-bearing majoritic garnet, hand-picked under a reflected light microscope were examined with a Bruker-Enraf MACH3 single-crystal diffractometer using graphite-monochromatized $MoK\alpha_1$ radiation. Some of them showing the best diffraction quality were chosen for the data collection, which was done at Università di Firenze, Italy, with an Oxford Diffraction Xcalibur 3 diffractometer (X-ray MoKα radiation, $\lambda = 0.71073$ Å) fitted with a Sapphire 2 CCD (Bindi et al., 2011).

3. EXPERIMENTAL RESULTS

3.1. Synthesis of pure sodium majorite $Na_2MgSi_5O_{12}$ and the Na-pyroxene/Na-majorite transition

The phase transition $NaMg_{0.5}Si_{2.5}O_6$ pyroxene/$Na_2MgSi_5O_{12}$ majorite was studied in the pressure range of 13–20 GPa at 1500–2100 °C. Conditions and results of experiments are given in Table 2. Depending on $P-T$ parameters, the main phases obtained in experiments are Na-pyroxene or Na-majorite (Fig. 3). Their concentration in run products is ⩾90 vol.%. The phases were distinguished by the values of *d*-spacing and intensities of the corresponding X-ray peaks on the powder XRD patterns (Dymshits et al., 2010).

Na-pyroxene forms relatively large idiomorphic crystals of prismatic habit with a size of up to 50 μm (Fig. 3a), sometimes in a fine-granular stishovite mass. Electron

Table 2
Conditions and results of the synthesis of Na-pyroxene ($NaMg_{0.5}Si_{2.5}O_6$) and Na-majorite ($Na_2MgSi_5O_{12}$).

Run No.	P (GPa)	T (°C)	Duration (min)	Products of synthesis
T1789a	13	1700	240	NaPx, St
T1811	14	1500	360	NaPx, St
T1789	14.5	1700	240	NaPx, St
ES237	15	1700	30	NaPx, St
T1810	16	1500	360	NaMaj, St
T1808	16	1900	120	NaPx, St
T1797	17	1700	30	NaMaj, St
ES238	17.5	1700	1440	NaMaj, St
T1812	17.5	1900	120	NaMaj, St
T1814	20	2100	30	NaMaj, St

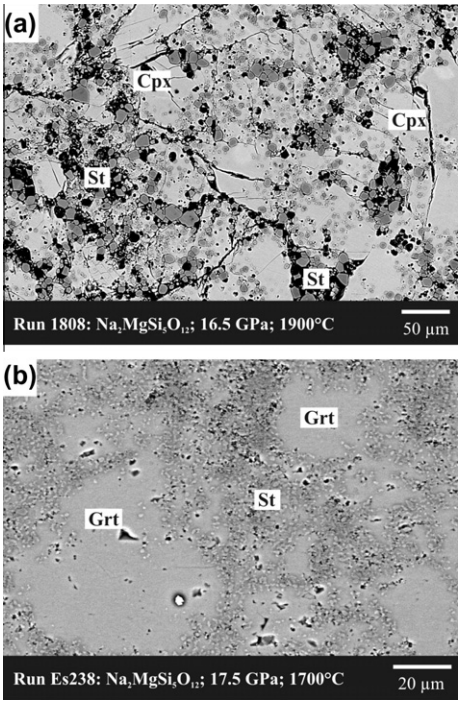

Fig. 3. BSE images of the samples with Na-pyroxene (a) and Na-majorite (b). Stishovite occurs in interstitials in both samples.

microprobe analyses of this mineral (wt.%, SiO_2 74.64; MgO 10.09; Na_2O 15.33; total 100.06) demonstrate its closeness to ideal stoichiometric composition $Na_{0.995}Mg_{0.503}Si_{2.500}O_{6.000}$. Na-majorite crystals of isometric shape with sizes of up to 50 μm are overgrown by smaller (up to 5 μm) grains from edges forming fine-granular interstitial aggregate together with stishovite (Fig. 3b). The largest garnet aggregates (up to 100 μm) were obtained in the long-time run (ES-238, 1440 min). Their composition (wt.%, SiO_2 75.32; MgO 10.11; Na_2O 15.08; total 100.51; formula $Na_{1.944}Mg_{1.003}Si_{5.013}O_{12.000}$) is also quite close to ideal stoichiometric composition. In some runs (e.g., 1810) incorporation of a small admixture of majoritic component ($Mg_4Si_4O_{12}$) is assumed judging from higher magnesium concentration in some grains (up to 1.273 f.u. Mg) and lower content of Si (up to 4.911 f.u.) relative to 5.000 per formula unit.

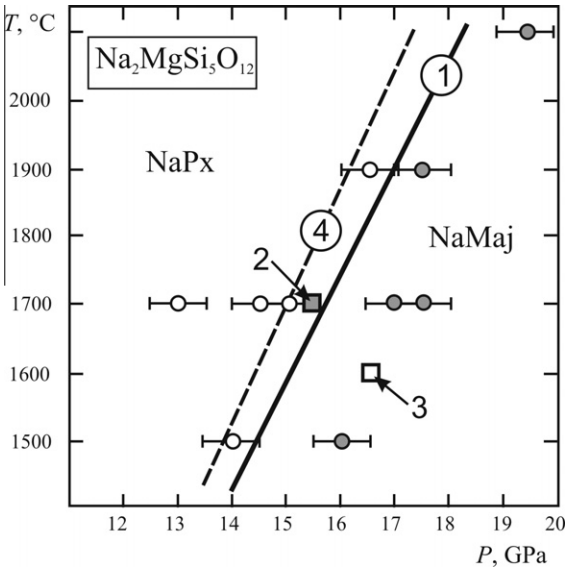

Fig. 4. Phase diagram demonstrating the stability of Na-pyroxene (empty circles) and Na-majorite (dark circles) in P–T coordinates. The accuracy of pressure measurement is indicated by horizontal bars. A solid line (1) illustrates the assumed phase boundary. The data on Na-majorite syntheses from (Gasparik, 1989) (2), (Pacalo et al., 1992) (3), as well as the results of *ab initio* computer simulations (Vinograd et al., 2011) (4) are shown for comparison.

The results of performed experiments allowed us to plot $P-T$ phase diagram (Fig. 4) demonstrating the fields of Na-pyroxene and Na-garnet stability. The phase boundary is fitted by the equation P (GPa) = 0.0050(2) T (°C) + 7.5(4) and has quite steep slope, because the first appearance of garnet is observed at a pressure of 16 GPa and a temperature of 1500 °C; garnet is formed at 1900 °C with increase of pressure up to 17.5 GPa. Note that the garnet stability was followed up to 19.5 GPa (2100 °C). The stability of this phase at higher $P-T$ is not confirmed yet. However, by the analogy with pyrope and majorite, we may assume its decomposition at pressures above 20–22 GPa with the formation of $MgSiO_3$ perovskite and sodium-rich silicate (Bobrov et al., 2008a).

3.2. Phase relations in the $Mg_3Al_2Si_3O_{12}$–$Na_2MgSi_5O_{12}$ join at 11–20 GPa

The conditions and results of high-pressure experiments on the pyrope ($Mg_3Al_2Si_3O_{12}$)–Na-majorite ($Na_2MgSi_5O_{12}$) system are summarized in Table 3, and the phase relations for this join are illustrated in Fig. 5. Phase assemblages and textural features of experimental samples are shown in Fig. 6. The temperatures of solidus and liquidus, as well as the T–X sections at $P = 7.0$ and 8.5 GPa were studied by Bobrov et al. (2008b). As it is evident from our experiments, the liquidus temperature at 11 GPa is ~2000 °C increasing up to ~2400 °C at 20 GPa. The slope of the liquidus line is positive over the studied pressure range. Slope of the solidus curve is also positive, however, being more

Table 3
Conditions and results of experiments in the $Mg_3Al_2Si_3O_{12}$–$Na_2MgSi_5O_{12}$ system.

Run	$Na_2MgSi_5O_{12}$	T (°C)	P (GPa)	Phases
T1803	50	2350	20	L
T1802	50	2300	20	Grt, St, L
T1804	50	2100	20	Grt, St
T1796	50	1800	19	Grt, CF, St
Es-241	80	1600	18.5	Grt, CF, St
Es-241	60	1600	18.5	Grt, CF, St
T1801	50	1600	18.5	Grt, CF, St
Es-241	40	1600	18.5	Grt, CF, St
Es-241	20	1600	18.5	Grt, St
T1812	50	1900	18	Grt, St
T1798	50	1900	17	Grt, St
T1808	50	1900	16	Px, Grt, St
T1810	50	1500	16	Grt, St
T1799	50	2200	15	Px, Grt, St, L
Es-243	50	2000	15	Px, Grt, St
T1805	50	1900	15	Px, Grt, St
T1795	50	1800	14	Px, Grt, St
T1811	50	1500	14	Px, Grt, St
T1813	50	1930	11	Px, Grt, Cs, L
T1800	50	1800	11	Px, Grt, Cs

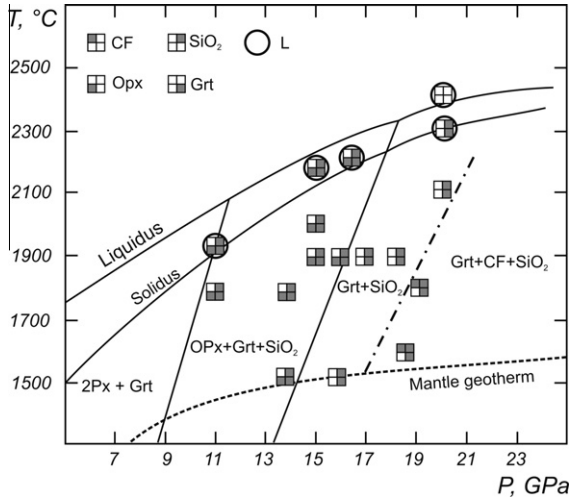

Fig. 5. P–T phase diagram of the $Mg_3Al_2Si_3O_{12}$–$Na_2MgSi_5O_{12}$ join for the composition of $Prp_{50}NaMaj_{50}$ (mol.%).

steep, so that the estimated partial melting range is ~200 °C at 9 GPa and <100 °C at 20 GPa.

Construction of the diagram in the low-pressure area is based on the results obtained in previous studies (Gasparik, 1989; Bobrov et al., 2008b). As shown by Bobrov et al. (2008b), the three-phase subsolidus assemblage (2Px + Grt) was formed in the pyrope–Na-majorite system above 1600 °C at 7–8.5 GPa. Two pyroxene solid solutions may coexist in this area (enstatite-rich and Na-pyroxene NaPx), since the solubility of jadeite (Jd) in En and NaPx in Jd is extensive at 7 GPa, whereas the solubility of NaPx is very limited. It was demonstrated by Angel et al. (1988) that NaPx $NaMg_{0.5}Si_{2.5}O_6$ contained both tetrahedrally and octahedrally coordinated silicon and hence its participation in the pyroxene solid solution was possible only at high pressures.

At $P \geqslant 11$ GPa under subsolidus conditions we obtained the three-phase assemblage of pyroxene, garnet, and coesite (Fig. 6a); the latter was replaced by stishovite at higher pressures (Fig. 6b). Garnet in all samples is enriched in silicon and sodium (majorite and Na-majorite components, Table 4). Pyroxene has a monoclinic symmetry being represented by the jadeite–Na-pyroxene–clinoenstatite solid solution. The concentration of jadeite increases with pressure, which is accompanied by increase of the portion of majoritic garnet in run products. The highest Na-pyroxene content in the pyroxene composition was registered at 15 GPa and 2000 °C. The portion of pyroxene in experimental samples progressively decreases from ~10 vol.% (11 GPa) to a few grains (16 GPa). The transition from the three-phase (Grt + Px + St) to the two-phase (Grt + St) field was established by disappearance of monoclinic pyroxene and the position of the boundary curve on the phase diagram is shown with account for the data on Na-pyroxene/Na-majorite phase transition (Fig. 4). The field (Grt + St) is characterized by the lowest content of St (<5 vol.%) (Fig. 6c).

Appearance of a high-sodium phase with the composition close to $NaAlSiO_4$ and the structure of calcium ferrite type (CF-phase) was registered in two runs (T1796 and T1801) performed at 18.5 and 19 GPa. CF occurred as small grains together with stishovite in interstitials between majoritic garnets or formed small inclusions in them (Fig. 6d). This allowed us to distinguish the three-phase field (Grt + CF + St) on the phase diagram (Fig. 5). Such association was previously obtained by Bobrov et al. (2008a) in the study of the model diopside–jadeite system at a pressure >22 GPa. CF in our runs contains up to 4.52 wt.% MgO due to the formation of the solid solution in the compositional range of $(1–x)NaAlSiO_4 \cdot xMgAl_2O_4$ ($0 \leqslant x \leqslant 0.3$), as it is evident from the experimental data (Ono et al., 2009).

3.3. Compositional and structural changes of majoritic garnet in the $Mg_3Al_2Si_3O_{12}$–$Na_2MgSi_5O_{12}$ join

Garnets synthesized in melting experiments have euhedral shape and grain size up to 50 μm, whereas garnets obtained in subsolidus experiments are subhedral with sizes up to 100 μm. All garnets are characterized by a stable sodium admixture and silicon surplus over 3.0 per f.u. (Table 4). They show a positive correlation of the Na content with Si (Fig. 7a) and a negative correlation of the Al content with Si (Fig. 7b), which provide evidence for the pressure-dependent substitution $Na^X + Si^Y = Mg^X + Al^Y$ (e.g., Ono and Yasuda, 1996; Bobrov et al., 2008b) and sodium incorporation in garnet as $Na_2MgSi_5O_{12}$ (sodium majorite) component (Fig. 7a).

For a given bulk composition ($Prp_{50}NaMaj_{50}$), we observe regular increase of both Na and Si concentrations and, consequently, NaMaj mole fraction in garnets (Fig. 8a). From 8.5 GPa (Bobrov et al., 2008b) to 20 GPa, the concentration of Na_2O changes from 1.52 to 5.71 wt.%, which corresponds to a NaMaj content of

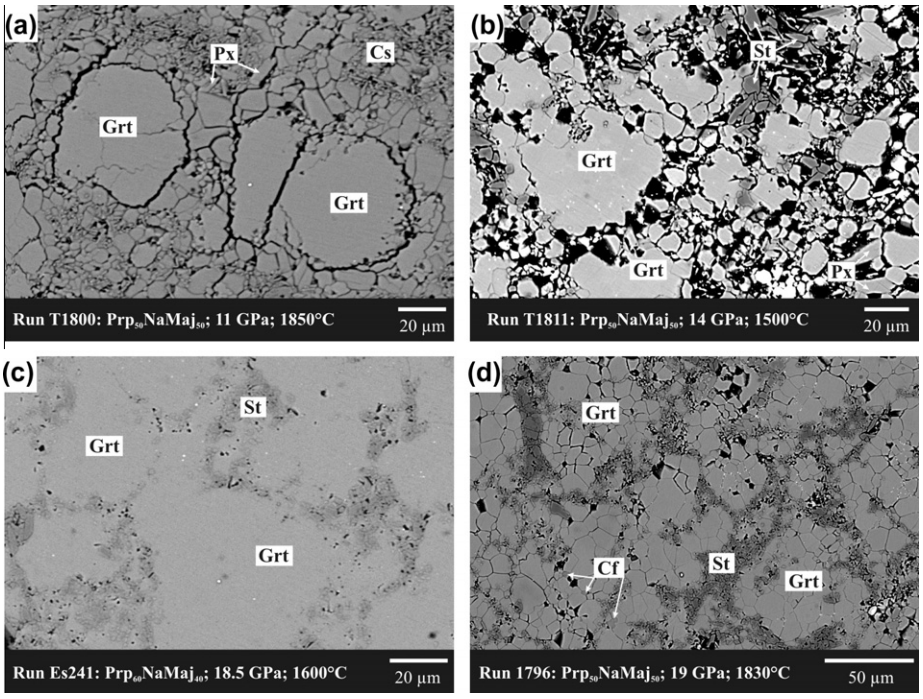

Fig. 6. Back-scattered electron images of textural relationships in some run products in the system $Mg_3Al_2Si_3O_{12}$–$Na_2MgSi_5O_{12}$ at 11–19 GPa. (a) Euhedral majoritic garnet crystals in the matrix of clinopyroxene and coesite grains; (b) aggregate of majoritic garnet, pyroxene, and stishovite; (c) euhedral majoritic garnet crystals with interstitial small acicular stishovite grains; (d) aggregate of majoritic garnet and $NaAlSiO_4$ with a calcium-ferrite structure and small acicular stishovite crystals in interstitials.

~40 mol.%. This results from gradual decrease of the content of Na-pyroxene in the run products, which is progressively dissolved in garnet. Hence the results of experiments performed for the $Prp_{50}NaMaj_{50}$ starting composition allow us to postulate the existence of the complete series of the pyrope–Na-majorite solid solution up to at least 40 mol.% $Na_2MgSi_5O_{12}$ (Fig. 8a). Further increase of sodium and silicon contents in garnet (up to 50 mol.% NaMaj) are expected at higher pressure, until $Na_2MgSi_5O_{12}$ is completely dissolved in garnet.

Some experiments performed under the conditions of partial melting allowed us to obtain the equilibrium phase assemblage of majoritic garnet and melt (Table 3). The content of the melt ranges from <5 to ~20 vol.% increasing with temperature. Melts are characterized by the lower concentrations of aluminum and high concentrations of silicon and sodium. This fact is consistent with the results of experiments in the pyrope–Na-majorite system at 7.0–8.5 GPa (Bobrov et al., 2008b), for which it was concluded that Na-bearing majoitic garnet is compatible with sodium-rich alkaline aluminosilicate melts due to the significant Na partitioning to melt with respect to majoritic garnet. However the Na partitioning coefficient between garnet and melt increases with pressure from 0.111 at 8.5 GPa to 0.328 and 0.608 at 15 and 20 GPa, respectively.

A special run (Es-241) was performed at 18.5 GPa and 1600 °C in a large volume cell and allowed us to study four different starting compositions ($Prp_{20}NaMaj_{80}$, $Prp_{40}NaMaj_{60}$, $Prp_{60}NaMaj_{40}$, and $Prp_{80}NaMaj_{20}$) under the same *PT*-parameters (Table 4). All samples contain NaMaj and small portions of St and CF (each <5 vol.%). Compositions of garnets synthesized in this run are shown in Table 5 and Fig. 8b. The concentrations of Na_2O and SiO_2 in garnet progressively increase with increase of the $Na_2MgSi_5O_{12}$ content in the starting materials reaching 12.24 and 69.22 wt.%, respectively ($Prp_{20}NaMaj_{80}$). This provides evidence for the formation of complete series of solid solutions in the system of sodium-bearing majoritic garnets ($Mg_3Al_2Si_3O_{12}$–$Na_2MgSi_5O_{12}$), similarly to the pyrope–majorite system (Akaogi and Akimoto, 1977).

The determined compositions of synthesized phases (Table 5) are almost identical with those of the starting materials and are on the join $Mg_3Al_2Si_3O_{12}$–$Na_2MgSi_5O_{12}$. Based on this data, the lattice parameters of the homogeneous solid solutions are plotted against compositions of the starting materials in Fig. 9. It is evident that the lattice parameters decrease linearly with increasing amount of $Na_2MgSi_5O_{12}$. All these garnet solid solutions synthesized from $Prp_{80}NaMaj_{20}$ to $Prp_{40}NaMaj_{60}$ have a cubic symmetry. There are clearly two peaks for the sample $Prp_{20}NaMaj_{80}$ instead of the one expected for a cubic material. This indicates that garnets with $Na_2MgSi_5O_{12}$ content of at least $\geqslant$80 mol.% possess tetragonal symmetry, which is in a good agreement with our recent study (Bindi et al., 2011). Detailed study of pure Na-majorite by single-crystal X-ray diffraction allowed us to establish that this phase has tetragonal symmetry with a space group $I4_1/acd$ and the lattice parameters $a = 11.3966(6)$, $c = 11.3369(5)$ Å, $V = 1472.5(1)$ Å^3.

Table 4
Compositions of phases synthesized in the pyrope–Na-majorite system (starting composition $Prp_{50}NaMaj_{50}$) at 11–20 GPa and 1500–2300 °C.

Run	T1813			T1800		T1795		1799	
P, GPa (*T*, °C)	11 (1930)			11 (1800)		14 (1800)		15 (2200)	
Phase	Grt	Px	L	Grt	Px	Grt	Px	Grt	L
SiO_2	48.54	58.77	67.10	49.33	59.45	49.81	60.97	54.67	60.52
Al_2O_3	19.53	6.42	8.03	19.31	6.64	20.93	5.01	18.13	15.62
MgO	29.31	29.95	11.97	28.57	28.10	27.93	29.31	25.03	13.02
Na_2O	1.64	3.17	13.30	1.80	4.92	2.19	4.52	3.59	10.84
Total	99.02	98.31	100.00	99.01	99.11	101.86	99.81	101.42	100.00
Formula units									
Si	3.294	1.997	4.469	3.343	2.012	3.315	2.046	3.584	4.034
Al	1.562	0.257	0.630	1.543	0.265	1.641	0.198	1.401	1.226
Mg	2.963	1.516	1.190	2.884	1.417	2.768	1.465	2.445	1.342
Na	0.216	0.209	1.711	0.236	0.323	0.282	0.294	0.559	1.398
Total	8.035	3.979	8.000	8.006	4.017	8.006	4.003	7.989	8.000

Run	T1808		T1796		1798	1812	T1804	T1802	
P, GPa (*T*, °C)	16 (1900)		19 (1800)		17 (1900)	18 (1900)	20 (2100)	20 (2300)	
Phase	Grt	Px	Grt	CF	Grt	Grt	Grt	Grt	L
SiO_2	54.67	59.71	54.72	40.97	53.93	55.99	56.66	55.43	62.44
Al_2O_3	17.13	17.70	17.03	35.41	17.02	16.15	14.57	14.36	7.15
MgO	25.03	9.35	24.83	3.86	24.61	23.95	23.52	23.33	20.93
Na_2O	4.49	11.61	4.60	18.67	4.96	5.32	5.71	5.55	9.33
Total	101.32	98.37	101.18	98.91	100.52	101.41	100.46	98.67	99.85
Formula units									
Si	3.619	2.037	3.628	0.973	3.607	3.705	3.785	3.771	4.158
Al	1.337	0.711	1.330	0.991	1.341	1.259	1.147	1.151	0.561
Mg	2.468	0.457	2.452	0.136	2.452	2.360	2.340	2.364	2.075
Na	0.577	0.768	0.591	0.859	0.643	0.682	0.739	0.732	1.204
Total	8.001	3.993	8.001	2.959	8.043	8.006	8.011	8.018	7.998

Run	ES-243		T1801		T1811		T1810	T1805	
P, GPa (*T*, °C)	15 (2000)		18.5 (1600)		14 (1500)		16 (1500)	15 (1900)	
Phase	Grt	Px	Grt	CF	Grt	Px	Grt	Grt	Px
SiO_2	54.86	59.62	55.01	35.52	47.94	59.83	54.72	54.83	59.25
Al_2O_3	15.67	4.65	17.18	41.31	22.40	4.15	16.20	17.12	5.60
MgO	27.07	28.65	24.03	4.52	27.99	33.01	26.13	25.86	29.32
Na_2O	3.72	4.53	4.74	18.33	1.66	3.24	4.31	4.08	4.58
Total	101.33	97.44	100.96	99.68	99.99	100.23	101.36	101.89	98.75
Formula units									
Si	3.630	2.026	3.652	0.836	3.220	1.994	3.625	3.607	2.015
Al	1.222	0.186	1.344	1.144	1.773	0.163	1.264	1.327	0.224
Mg	2.668	1.450	2.376	0.158	2.803	1.640	2.573	2.535	1.485
Na	0.477	0.298	0.609	0.835	0.216	0.209	0.553	0.520	0.298
Total	7.997	3.960	7.981	2.973	8.012	4.006	8.015	7.989	4.022

4. DISCUSSION OF THE RESULTS

4.1. Implications for the upper mantle and transition zone

The $Mg_3Al_2Si_3O_{12}$–$Na_2MgSi_5O_{12}$ join is of particular relevance to Na incorporation in majoritic garnet, since it proceeds according to the Mg + Al = Na + Si substitution (Irifune, 1987; Gasparik, 1996; Ono and Yasuda, 1996; Bobrov et al., 2008a,b). This substitution may be illustrated on the triangle (Fig. 10), where $Mg_2NaAlSi_4O_{12}$ would correspond to an intermediate composition along the $Mg_3Al_2Si_3O_{12}$–$Na_2MgSi_5O_{12}$ join. It should be noted that the average MORB composition plots close to this compositional join and therefore the results obtained in this study have direct implications for natural eclogitic majoritic garnets observed as inclusions in diamonds.

Stachel et al. (2000) and Harte and Cayzer (2007) suggested that diamonds containing majoritic garnets were formed under the conditions of the lowermost upper mantle and transition zone at pressures of 10–15 GPa. An idea of subduction-related origin of diamonds from the asthenosphere and transition zone may provide an explanation for the almost exclusively eclogitic paragenesis of their inclusions. Different subduction levels are characterized

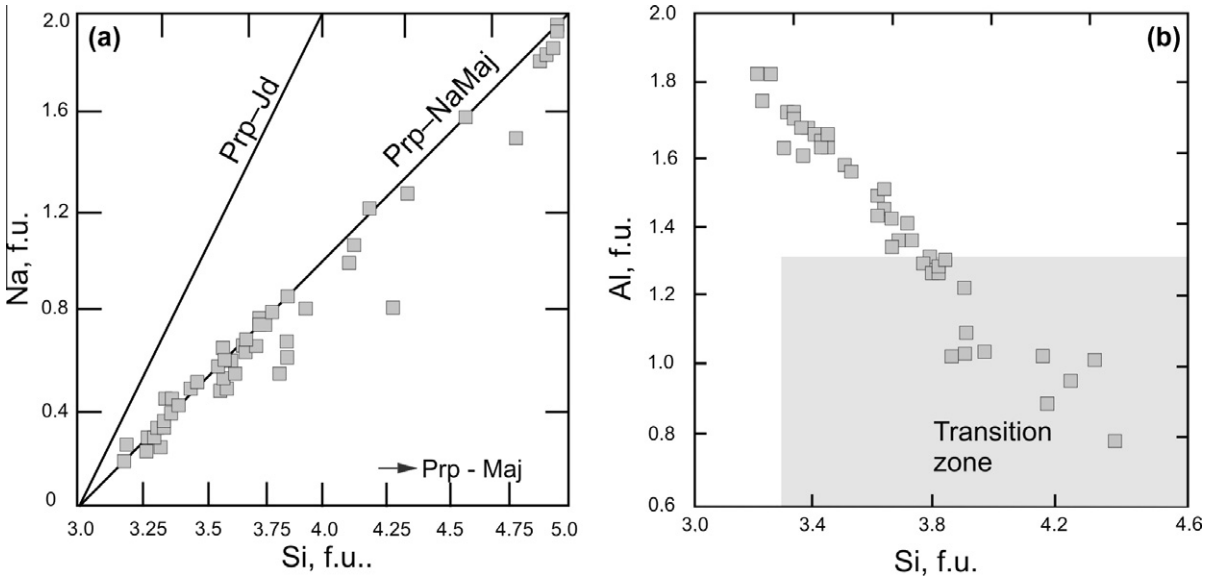

Fig. 7. Na vs. Si (a) and Al vs. Si (b) diagrams of the compositions of Na-bearing majoritic garnets synthesized in experiments in the system $Mg_3Al_2Si_3O_{12}$–$Na_2MgSi_5O_{12}$ at 11–19 GPa.

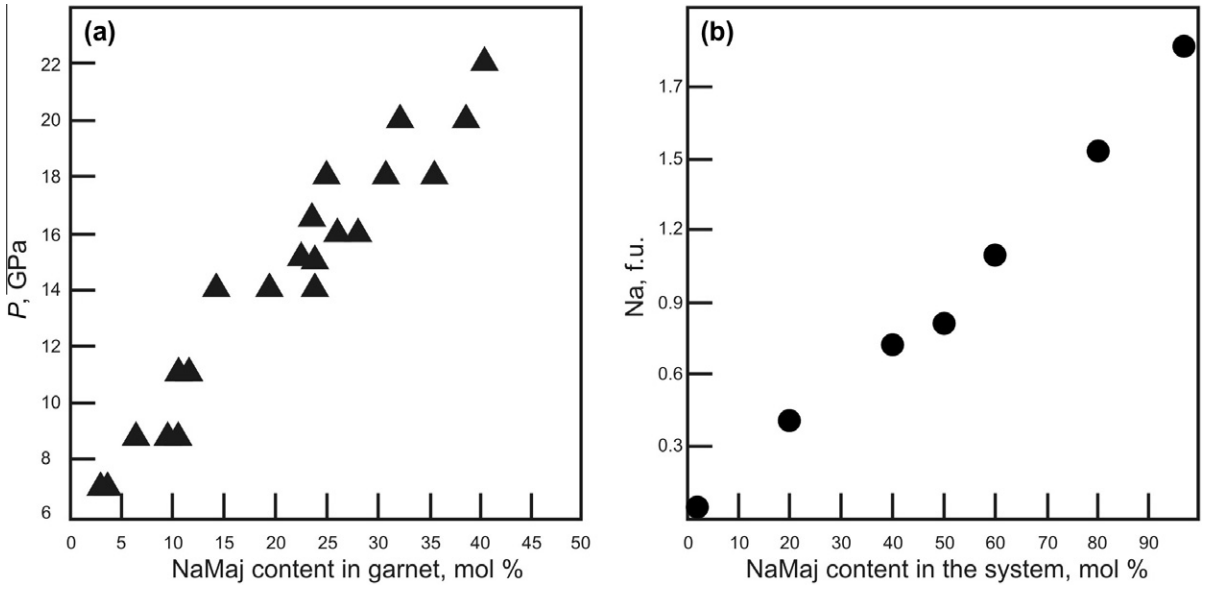

Fig. 8. Compositions of garnets synthesized in experiments. (a) Dependence of Na-majorite content in garnets on pressure for the $Prp_{50}NaMaj_{50}$ starting composition; (b) linear correlation between the Na (a.p.f.u.) concentration in garnet and the NaMaj content in the starting materials demonstrating the complete series of solid solutions in the $Mg_3Al_2Si_3O_{12}$–$Na_2MgSi_5O_{12}$.

by various mineral assemblages, which are well documented by phase transformations in the eclogitic system. Numerous experimental studies were performed to investigate the compositional evolution of garnet, pyroxene, and other phases in bulk compositions that produce eclogitic assemblages in a broad sense covering virtually all relevant *P–T* conditions of the Earth's interior (e.g., Yasuda et al., 1994; Ono and Yasuda, 1996; Okamoto and Maruyama, 1998, 2004; Hirose and Fei, 2002; Kessel et al., 2005; Litasov and Ohtani, 2005; Bobrov et al., 2008a). However, the physicochemical behavior of sodium components of minerals in magmatic processes under mantle pressures and temperatures is not well studied.

Currently new results on the synthesis of sodium-bearing compounds with silicon in octahedral coordination were obtained, which is reliable evidence for their ultrahigh pressure formation. Among them are $Na_2Si(Si_2O_7)$ (Fleet and Henderson, 1995), $Na_{1.8}Ca_{1.1}Si_6O_{14}$ (Gasparik et al., 1995), $Na_6Si_3(Si_9O_{27})$ (Fleet, 1996), $Na_8Si(Si_6O_{18})$ (Fleet, 1998), $Na_2Mg_{4+x}Fe_{2-2x}^{3+}Si_{6+x}O_{20}$ (Gasparik et al., 1999), and $(K,Na)_{0.9}(Mg,Fe)_2(Mg,Fe,Al,Si)_6O_{12}$ (Gasparik et al., 2000). Sodium pyroxene $NaMg_{0.5}Si_{2.5}O_6$ (Angel et al.,

Table 5
Composition and cell parameters of garnets synthesized in the system $Mg_3Al_2Si_3O_{12}$– $Na_2MgSi_5O_{12}$ at 17.5 GPa and 1600 °C.

Composition	1	2	3	4
SiO_2	51.20	57.21	63.21	69.22
Al_2O_3	20.26	15.16	10.06	4.97
MgO	26.11	22.28	17.94	14.31
Na_2O	3.18	6.12	9.45	12.24
Total	100.75	100.77	100.66	100.75
Formula units				
Si	3.410	3.810	4.210	4.610
Al	1.590	1.190	0.790	0.390
Mg	2.590	2.210	1.780	1.420
Na	0.410	0.790	1.220	1.580
Total	8.000	8.000	8.000	8.000
Lattice parameter (Å)	a = 11.4395(4)	a = 11.4245(5)	a = 11.4090(4)	a = 11.4003(5) c = 11.3851(3)

Starting compositions: (1) $Prp_{80}NaMaj_{20}$; (2) $Prp_{60}NaMaj_{40}$; (3) $Prp_{40}NaMaj_{60}$; (4) $Prp_{20}NaMaj_{80}$.

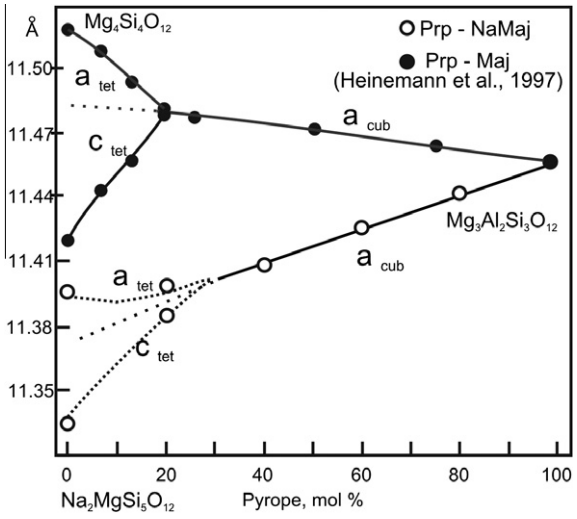

Fig. 9. Variations of unit cell parameters as a function of composition for a series of phases along the pyrope ($Mg_3Al_2Si_3O_{12}$)–Na-majorite ($Na_2MgSi_5O_{12}$) garnet join. The values for the pyrope end member composition are taken from Parise et al. (1996); Na-majorite, from Bindi et al. (2011). Variations of unit cell parameters for the pyrope–majorite ($Mg_4Si_4O_{12}$) series (Parise et al., 1996) are shown for comparison.

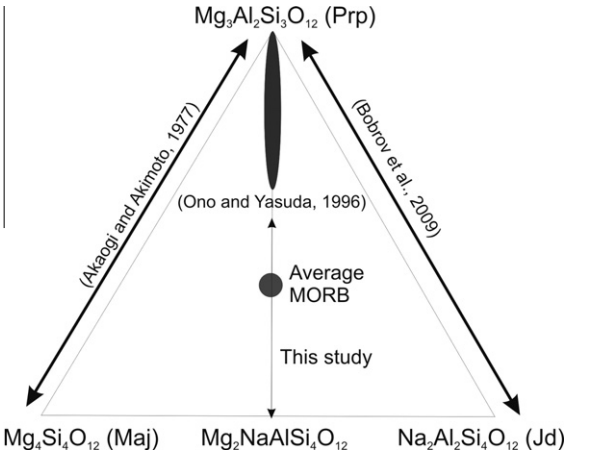

Fig. 10. Composition of the studied system in comparison with previously studied systems containing Na-bearing majoritic garnet and MORB composition. (See above-mentioned references for further information.)

1988) and its solid solutions with the composition of $Na(Mg_xSi_xAl_{1-2x})Si_2O_6$ ($0 \leqslant x \leqslant 0.5$) (Yang et al., 2009), as well as sodium majorite $Na_2MgSi_5O_{12}$ (Pacalo et al., 1992; Dymshits et al., 2010; Bindi et al., 2011) and pyrope–Na-majorite solid solutions synthesized in this study should hold a certain place among the mentioned phases.

Na-bearing majoritic garnet should play a key role in discussion about high-pressure phases, which may be potential sodium concentrators in the lower parts of the upper mantle and transition zone. According to the existing concepts, for example, pyrolite model (Ringwood, 1991), the portion of garnet within the depth range from 410 to 660 km may exceed 50 vol.%. Calculations show that at a bulk concentration of ~0.4 wt.% Na_2O, the sodium content in garnet resulting from incorporation of the $Na_2MgSi_5O_{12}$ end-member in it will not exceed 0.8–0.9 wt.% Na_2O. If we accept the model of the layered structure of the mantle (Anderson, 1979), according to which eclogite being transformed to garnetite at a pressure of >18 GPa (Gasparik, 1989; Bobrov et al., 2008a) predominates at the base of the upper mantle and in the transition zone, garnet of these rocks will contain from ~1 to ~5 wt.% Na_2O depending on the bulk eclogite (garnetite) composition. It has been established experimentally that $Na_2MgSi_5O_{12}$ solubility is quite significant and exceeds 30 mol.% in pyrope–grossular garnet (Bobrov et al., 2008a). According to the data obtained in this study, there is complete series of solid solutions in the system of Na-bearing majoritic garnet and, therefore, the ability of the garnet phase to accumulate significant concentrations of sodium under the conditions of the lower parts of the upper mantle and transition zone is unambiguous.

P–T conditions of the Na-pyroxene/Na-majorite phase experimentally obtained in this study (Fig. 4) are compared with the results of previous independent studies of Na-majorite syntheses at 15.4 GPa (Gasparik, 1989) and 16.5 GPa (Pacalo et al., 1992) and our recent data on computer simulation of Na-majorite (Vinograd et al., 2011). The line obtained from calculations at 0 and 1923 K has almost the same slope being located very close (<1 GPa) from the Na-pyroxene/Na-garnet phase boundary obtained experimentally. As this takes place, computer simulations of high-pressure mineral assemblages including majoritic garnet may provide a reliable addition to the experimental studies, and could provide an independent tool for getting thermodynamic information in the field of deep mineralogy of the Earth.

4.2. Structural features of Na-bearing maforitic garnets

An important aspect of the Na-pyroxene/Na-majorite transformation is that the symmetry changes from monoclinic (similar to that of jadeite) in $NaMg_{0.5}Si_{2.5}O_6$ pyroxene to tetragonal in $Na_2MgSi_5O_{12}$ garnet. As was demonstrated by Bindi et al. (2011), both Y (octahedral) and Z (tetrahedral) sites of the Na-majorite structure are occupied by silicon, whereas Mg and Na are disordered at the X sites. In this case, we may expect decrease in the unit-cell parameters from $Na_2MgSi_5O_{12}$ to pure pyrope with decrease of sodium concentration. However, as it is evident from Fig. 9, the situation is opposite, which most likely is an obvious crystal-chemical response of the crystal structure.

The octahedral site is of special importance for the crystal-chemical variation. Passing from pure $Na_2MgSi_5O_{12}$ to pure pyrope ($Mg_3Al_2Si_3O_{12}$), we observe the transition from an octahedron fully occupied by silicon to an octahedron fully occupied by aluminum. The difference in their sizes is significant being much larger in pyrope. On the other hand, transition from Na-majorite to pyrope results in change from an X-site with a mixed (Na,Mg) population to an X-site fully occupied with Mg. The difference in their size in this crystal-chemical environment is not so significant. As a result, an increase of the unit-cell parameters is observed from $Na_2MgSi_5O_{12}$ to pure pyrope.

In Fig. 9 we observe the similarity between the Na-majorite–pyrope and majorite–pyrope solid solutions in relation to the tetragonal/cubic transition at the low pyrope content (~20 and 25 mol.% Prp). However, further increase of pyrope concentration in majoritic garnet results in decrease of the unit-cell parameters (Table 1). Majorite $Mg_4Si_4O_{12}$ (or $Mg_3(MgSi)Si_3O_{12}$) demonstrates the same environments in terms of X and Z sites as pyrope, so that the only difference is in the Y (octahedral) site. Majorite has a mixed (MgSi) Y site, whereas Y site of pure pyrope is occupied only by aluminum. Consequently, an octahedron fully hosted by Al is slightly larger than that hosted by Mg + Si. Indeed, the presence of Si in the Y-site drastically decreases the space filled by the Y-environment. In this case, transition from majorite to pyrope is accompanied by a slight decrease in the unit-cell parameters.

Single-crystal X-ray diffraction studies of different garnets at high pressures available for pyrope, grossular and andradite (Hazen and Finger, 1978, 1989; Levien et al., 1979) demonstrated that the compression of these garnets is controlled by the compressibility of the dodecahedral site. However, the study of the comparative compressibilities of garnets (Hazen et al., 1994) provided evidence for the different behavior of majoritic garnets. Thus, garnet with Na in dodecahedral site was found to be the least compressible among garnets, although the compressibility of Na is quite high. Our data on the Na-majorite structure provide an explanation of the low compressibility of $Na_2MgSi_5O_{12}$, as a component having the smallest cell parameters in comparison with majorite and pyrope.

5. CONCLUSION

The results of this study allowed us to model mineral transformations in the system $Mg_3Al_2Si_3O_{12}$–$Na_2MgSi_5O_{12}$ within the upper mantle and transition zone. As it is evident from our experiments, the composition and symmetry of garnet are clearly dependent on pressure and bulk composition. With respect to the understanding of the formation of Na-bearing majoritic garnets ($Mg_3Al_2Si_3O_{12}$–$Na_2MgSi_5O_{12}$ solid solutions), the successful synthesis of the $Na_2MgSi_5O_{12}$ end-member becomes especially important, because the determination of its thermodynamic constants in combination with the data of computer simulation will provide a better insight into the problem of the barometry of mineral associations with majoritic garnet.

ACKNOWLEDGMENTS

The constructive reviews by Ken Collerson, Oleg Safonov, and anonymous referee were very helpful for improving the quality of the manuscript. This study was supported by the Russian Foundation for Basic Research (projects 12-05-00426, 12-05-31351, 12-05-33044, and 11-05-00401), by the Foundation of the President of Russian Federation (grant MD-534.2011.5 for Young Doctors of Sciences and grant NSh-5877.2012.5 for Leading Scientific Schools), and Integration project No. 97 (Siberian Branch, Russian Academy of Sciences). The experiments were conducted as a part of the Tohoku University Global Center-of-Excellence program, Japan "Global Education and Research Center for Earth and Planetary Dynamics".

REFERENCES

Akaogi M. and Akimoto S. (1977) Pyroxene-garnet solid solution equilibria in the systems $Mg_4Si_4O_{12}$–$Mg_3Al_2Si_3O_{12}$ and $Fe_4Si_4O_{12}$–$Fe_3Al_2Si_3O_{12}$ at high pressures and temperatures. *Phys. Earth Planet. Interiors* **15**, 90–106.

Akaogi M. and Akimoto S. (1979) High-pressure phase equilibria in a garnet lherzolite, with special reference to Mg^{2+}–Fe^{2+} partitioning among constituent minerals. *Phys. Earth Planet. Interiors* **19**, 31–51.

Anderson D. L. (1979) Chemical stratification of the mantle. *J. Geophys. Res.* **84**, 6297–6298.

Angel R. J., Gasparik T., Ross N. L., Finger L. W., Prewitt C. T. and Hazen R. M. (1988) A silica-rich sodium pyroxene phase with six-coordinated silicon. *Nature* **335**, 156–158.

Bindi L., Dymshits A. M., Bobrov A. V., Litasov K. D., Shatskiy A. F., Ohtani E. and Litvin Yu. A. (2011) Crystal chemistry of sodium in the Earth's interior: the structure of $Na_2MgSi_5O_{12}$ synthesized at 17.5 GPa and 1700 °C. *Am. Mineral.* **96**, 447–450.

Bobrov A. V., Dymshits A. M. and Litvin Yu. A. (2009) Conditions of magmatic crystallization of Na-bearing majoritic garnets in the Earth mantle: evidence from experimental and natural data. *Geochem. Int.* **47**, 951–965.

Bobrov A. V., Kojitani H., Akaogi M. and Litvin Yu. A. (2008a) Phase relations on the diopside–hedenbergite–jadeite join up to 24 GPa and stability of Na-bearing majoritic garnet. *Geochim. Cosmochim. Acta* **72**, 2392–2408.

Bobrov A. V., Litvin Yu. A., Bindi L. and Dymshits A. M. (2008b) Phase relations and formation of sodium-rich majoritic garnet in the system $Mg_3Al_2Si_3O_{12}$–$Na_2MgSi_5O_{12}$ at 7.0 and 8.5 GPa. *Contrib. Mineral. Petrol.* **156**, 243–257.

Collerson K. D., Williams Q., Kamber B. S., Omori S., Arai H. and Ohtani E. (2010) Majoritic garnet: a new approach to pressure estimation of shock events in meteorites and the encapsulation of sub-lithospheric inclusions in diamond. *Geochim. Cosmochim. Acta* **74**, 5939–5957.

Davies R. M., Griffin W. L. and O'Reilly S. Y. (1999) Diamonds from the deep: pipe DO27, Slave craton, Canada. In: *Proc. of the VII Intern. Kimb. Conf. Cape Town, Red Roof Design*, vol. 1 (eds. J. J. Gurney, J. L. Gurney, M. D. Pascoe and S. H. Richardson), pp. 148–155.

Davies R. M., Griffin W. L., O'Reilly S. Y. and McCandless T. E. (2004) Inclusions in diamonds from the K14 and K10 kimberlites, Buffalo Hills, Alberta, Canada: diamond growth in a plume? *Lithos* **77**, 99–111.

Dymshits A. M., Bobrov A. V., Litasov K. D., Shatskiy A. F., Ohtani E. and Litvin Yu. A. (2010) Experimental study of the pyroxene–garnet phase transition in the $Na_2MgSi_5O_{12}$ system at pressures of 13–20 GPa: first synthesis of sodium majorite. *Doklady Earth Sci.* **434**(1), 1263–1266.

Fei Y., Ricolleau A., Frank M., Mibe K., Shen G. and Prakapenka V. (2007) Toward an internally consistent pressure scale. *Proc. Natl. Acad. Sci. USA* **104**, 9182–9186.

Fleet M. E. (1996) Sodium tetrasilicate: a complex high-pressure framework silicate ($Na_6Si_3[Si_9O_{27}]$). *Am. Mineral.* **83**, 618–624.

Fleet M. E. (1998) Sodium heptasilicate: a high-pressure silicate with six-membered rings of tetrahedra interconnected by SiO_6 octahedra: $[Na_8Si(Si_6O_{18})]$. *Am. Mineral.* **83**, 618–624.

Fleet M. E. and Henderson G. S. (1995) Sodium trisilicate – a new high-pressure silicate structure $[Na_2Si(Si_2O_7)]$. *Phys. Chem. Mineral.* **22**, 383–386.

Frost D. J., Poe B. T., Tronnes R. G., Liebske C., Duba A. and Rubie D. C. (2004) A new large-volume multianvil system. *Phys. Earth Planet. Interiors* **143**, 507–514.

Gasparik T. (1989) Transformation of enstatite–diopside–jadeite pyroxenes to garnet. *Contrib. Mineral. Petrol.* **102**, 389–405.

Gasparik T. (1992) Enstatite–jadeite join and its role in the Earth's mantle. *Contrib. Mineral. Petrol.* **111**, 283–298.

Gasparik T. (1996) Diopside–jadeite join at 16–22 GPa. *Phys. Chem. Mineral.* **23**, 476–486.

Gasparik T. (2002) Experimental investigations of the origin of majoritic garnet inclusions in diamonds. *Phys. Chem. Mineral.* **29**, 170–180.

Gasparik T., Parise J. B., Eiben B. A. and Hriljac J. A. (1995) Stability and structure of a new high-pressure silicate, $Na_{1.8}Ca_{1.1}Si_6O_{14}$. *Am. Mineral.* **80**, 1269–1276.

Gasparik T., Parise J. B., Reeder R. J., Young V. G. and Wilford W. S. (1999) Composition, stability, and structure of a new member of the aenigmatite group, $Na_2Mg_{4+x}Fe^{3+}_{2-2x}Si_{6+x}O_{20}$, synthesized at 13–14 GPa. *Am. Mineral.* **84**, 257–266.

Gasparik T., Tripathi A. and Parise J. B. (2000) Structure of a new Al-rich phase, $[K, Na]_{0.9}[Mg, Fe]_2[Mg, Fe, Al, Si]_6O_{12}$, synthesized at 24 GPa. *Am. Mineral.* **85**, 613–618.

Hamilton D. L. and Henderson C. M. B. (1968) The preparation of silicate compositions by a gelling method. *Mineral. Mag.* **36**, 832–838.

Harte B. and Cayzer N. (2007) Decompression and unmixing of crystals included in diamonds from the mantle transition zone. *Phys. Chem. Mineral.* **34**, 647–656.

Harte B., Harris J. W., Hutchison M. T., Watt G. R. and Wilding M. C. (1999) Lower mantle mineral associations in diamonds from São Luiz, Brazil. In *Mantle Petrology: Field Observations and High Pressure Experimentation: A Tribute to Francis R. (Joe) Boyd* (eds. Y. Fei, C. M. Bertka and B. O. Mysen). The Geochemical Society, Houston, pp. 125–153.

Hazen R. M., Downs R. T., Conrad P. G., Finger L. W. and Gasparik T. (1994) Comparative compressibilities of majorite-type garnets. *Phys. Chem. Mineral.* **21**, 344–349.

Hazen R. M. and Finger L. W. (1978) Crystal structures and compressibilities of pyrope and grossular to 60 kbar. *Am. Mineral.* **63**, 297–303.

Hazen R. M. and Finger L. W. (1989) High-pressure crystal chemistry of andradite and pyrope: revised procedures for high-pressure diffraction experiments. *Am. Mineral.* **74**, 352–359.

Heinemann S., Sharp T. G., Seifert F. and Rubie D. C. (1997) The cubic-tetragonal phase transition in the system majorite ($Mg_4Si_4O_{12}$)–pyrope ($Mg_3Al_2Si_3O_{12}$), and garnet symmetry in the Earth's transition zone. *Phys. Chem. Mineral.* **24**, 206–221.

Hirose K. and Fei Y. W. (2002) Subsolidus and melting phase relations of basaltic composition in the uppermost lower mantle. *Geochim. Cosmochim. Acta* **66**, 2099–2108.

Irifune T. (1987) An experimental investigation of the pyroxene-garnet transformation in a pyrolite composition and its bearing on the constitution of the mantle. *Phys. Earth Planet. Interiors* **45**, 324–336.

Irifune T., Sekine T., Ringwood A. E. and Hibberson W. O. (1986) The eclogite–garnetite transformation at high pressure and some geophysical implications. *Earth Planet. Sci. Lett.* **77**, 245–256.

Irifune T. and Ringwood A. E. (1993) Phase transformations in subducted oceanic crust and buoyancy relationships at depths of 600–800 km in the mantle. *Earth Planet. Sci. Lett.* **117**, 101–110.

Kaminsky F. (2012) Mineralogy of the lower mantle: a review of 'super-deep' mineral inclusions in diamond. *Earth Sci. Rev.* **110**, 127–147.

Kaminsky F. V., Zakharchenko O. D., Davies R., Griffin W. L., Khachatryan-Blinova G. K. and Shiryaev A. A. (2001) Super-deep diamonds from the Juina area, Mato Grosso State, Brazil. *Contib. Mineral. Petrol.* **140**, 734–753.

Kessel R., Ulmer P., Pettke T., Schmidt M. W. and Thompson A. B. (2005) The water–basalt system at 4 to 6 GPa: phase relations and second critical endpoint in a K-free eclogite at 700 to 1400 °C. *Earth Planet. Sci. Lett.* **237**, 873–892.

Levien L., Prewitt C. T. and Weidner D. J. (1979) Compression of pyrope. *Am. Mineral.* **64**, 805–808.

Litasov K., Ohtani E., Suzuki A., Kawazoe T. and Funakoshi K. (2004) Absence of density crossover between basalt and peridotite in the cold slabs passing through 660 km discontinuity. *Geophys. Res. Lett.* **31**, L24607.

Litasov K. D. and Ohtani E. (2005) Phase relations in hydrous MORB at 18–28 GPa: implications for heterogeneity of the lower mantle. *Phys. Earth Planet. Interiors* **150**, 239–263.

Litasov K. D. and Ohtani E. (2009) Phase relations in the peridotite–carbonate–chloride system at 7.0–16.5 GPa and the

role of chlorides in the origin of kimberlite and diamond. *Chem. Geol.* **262**, 29–41.

Moore R. O. and Gurney J. J. (1985) Pyroxene solid solution in garnets included in diamonds. *Nature* **318**, 553–555.

Okamoto K. and Maruyama S. (1998) Multi-anvil re-equilibration experiments of a Dabie Shan ultrahigh-pressure eclogite within the diamond stability fields. *Island Arc* **7**, 52–69.

Okamoto K. and Maruyama S. (2004) The eclogite–garnetite transformation in the MORB + H_2O system. *Phys. Earth Planet. Interiors* **146**, 283–296.

Ono A., Akaogi M., Kojitani H., Yamashita K. and Kobayashi M. (2009) High-pressure phase relations and thermodynamic properties of hexagonal aluminous phase and calcium-ferrite phase in the systems $NaAlSiO_4$–$MgAl_2O_4$ and $CaAl_2O_4MgAl_2O_4$. *Phys. Earth Planet. Interiors* **174**, 39–49.

Ono S. and Yasuda A. (1996) Compositional change of majoritic garnet in a MORB composition from 7 to 17 GPa and 1400 to 1600 degrees C. *Phys. Earth Planet. Interiors* **96**, 171–179.

Pacalo R. E. G., Weidner D. J. and Gasparik T. (1992) Elastic properties of sodium-rich majorite garnet. *Geophys. Res. Lett.* **19**, 1895–1898.

Parise J. B., Wang Y., Gwanmesia G. D., Zhang J., Sinelnikov Y., Chmielowski J., Weidner D. J. and Liebermann R. C. (1996) The symmetry of garnets on the pyrope ($Mg_3Al_2Si_3O_{12}$)–majorite ($MgSiO_3$) join. *Geophys. Res. Lett.* **23**, 3799–3802.

Pokhilenko N. P., Sobolev N. V., Reutsky V. N., Hall A. E. and Taylor L. A. (2004) Crystalline inclusions and C isotope ratios in diamonds from the Snap Lake/King Lake kimberlite dyke system: evidence of ultradeep and enriched lithospheric mantle. *Lithos* **77**, 57–67.

Ringwood A. E. (1991) Phase transformations and their bearing on the constitution and dynamics of the mantle. *Geochim. Cosmochim. Acta* **55**, 2083–2110.

Ringwood A. E. and Major A. (1971) Synthesis of majorite and other high pressure garnets and perovskites. *Earth Planet. Sci. Lett.* **12**, 411–418.

Shatskii V. S., Zedgenizov D. A. and Ragozin A. L. (2010) Majoritic garnets in diamonds from placers of the Northeastern Siberian Platform. *Doklady Earth Sci.* **435**(2), 435–438.

Shatskiy A., Katsura T., Litasov K. D., Shcherbakova A. V., Borzdov Y. M., Yamazaki D., Yoneda A., Ohtani E. and Ito E. (2011) High pressure generation using scaled-up Kawai-cell. *Phys. Earth Planet. Interiors* **189**, 92–108.

Simakov S. K. and Bobrov A. V. (2008) Garnet–pyroxene barometry for the assemblages with Na-bearing majoritic garnet. *Doklady Earth Sci.* **420**, 667–669.

Sobolev N. V. and Lavrent'ev Y. G. (1971) Isomorphic sodium admixture in garnets formed at high pressures. *Contib. Mineral. Petrol.* **31**, 1–12.

Stachel T. (2001) Diamonds from the asthenosphere and the transition zone. *Eur. J. Mineral.* **13**, 883–892.

Stachel T., Harris J. W., Brey G. P. and Joswig W. (2000) Kankan diamonds (Guinea) I: from the lithosphere down to the transition zone. *Contrib. Mineral. Petrol.* **140**, 1–15.

Vinograd V. L., Dymshits A. M., Winkler B. and Bobrov A. V. (2011) Computer simulation of Na-bearing majoritic garnet. *Doklady Earth Sci.* **441**(1), 1508–1511.

Wilding M. C., Harte B. and Harris J. W. (1991) Evidence for a deep origin for the Sao Luiz diamonds. In *Fifth International Kimberlite Conference Extended Abstracts, Araxa*, pp. 456–458.

Yang H., Konzett J., Frost D. J. and Downs R. T. (2009) X-ray diffraction and Raman spectroscopic study of clinopyroxenes with six-coordinated Si in the $Na(Mg_{0.5}Si_{0.5})Si_2O_6$–$NaAlSi_2O_6$ system. *Am. Mineral.* **94**, 942–949.

Yasuda A., Fujii T. and Kurita K. (1994) Melting phase relations of an anhydrous mid-ocean ridge basalt from 3 to 20 GPa: implications for the behavior of abducted oceanic crust in the mantle. *J. Geophys. Res.* **99**(B5), 9401–9414.

Associate editor: Peter Ulmer